Behavior of *Trichoderma reesei* Hydrophobins in Solution: Interactions, Dynamics, and Multimer Formation†

Géza R. Szilvay,*,‡,§ Tiina Nakari-Setälä,‡ and Markus B. Linder‡

VTT Biotechnology, Tietotie 2, P.O. Box 1000, FIN-02044 VTT, Finland, and Program for Structural Biology and Biophysics, Institute of Biotechnology, University of Helsinki, FIN-00014, Helsinki, Finland

Received March 29, 2006; Revised Manuscript Received May 17, 2006

ABSTRACT: Filamentous fungi utilize small amphiphilic proteins called hydrophobins in their adaptation to the environment. The hydrophobins are used to form coatings on various fungal structures, lower the surface tension of water, and to mediate surface attachment. Hydrophobins function through self-assembly at interfaces, for example, at the air−water interface, and at fungal cellular structures. Despite their high tendency to self assemble at interfaces, hydrophobins can be very soluble in water. To understand the mechanism of hydrophobin self-assembly, in this work, we have studied the behavior of two *Trichoderma reesei* hydrophobins, HFBI and HFBII in aqueous solution. The main methods used were Förster resonance energy transfer (FRET) and size exclusion chromatography. A genetically engineered HFBI variant, NCys−HFBI, was utilized for the site-specific labeling of dyes for the FRET experiments. We observed the multimerization of HFBI in a concentration-dependent manner. A change from monomers to tetramers was seen when the hydrophobin concentration was increased. Interaction studies between HFBI and HFBII suggested that at low concentrations homodimers are preferred, and at higher concentrations, the heterotetramers of HFBI and HFBII are formed. In conclusion, the results support the model where hydrophobins in aqueous solutions form multimers by hydrophobic interactions. In contrast to micelles formed by detergents, the hydrophobin multimers are defined in size and involve specific protein−protein interactions.

Hydrophobins are a group of amphiphilic proteins found in filamentous fungi. They are small proteins of the size of approximately 70−120 amino acids (*1*, *2*). They were originally identified as genes that were very highly expressed in certain stages of growth. Studies on hydrophobins have shown that they can have a multitude of different roles and functions in fungal development. A common feature of the various functions of hydrophobins seems to involve interfacial phenomena in one way or another. For example, hydrophobins form coatings on fungal structures such as spores and fruiting bodies. They also lower the surface tension of water so that fungal hyphae can penetrate the air−water interface (*3*−*6*). Hydrophobins also have morphological roles (*7*) and are involved in fungal pathogen−host interactions (*8*, *9*). To perform these functions, hydrophobins have several extraordinary properties as surface active molecules. They adhere tightly to surfaces, form films on interfaces, and form foams efficiently because of their surface activity (*1*). Hydrophobins are among the most surface active proteins known (*2*, *10*, *11*). Because of their adhesive properties and surface activity, hydrophobins are interesting for biotechnical applications, for example, for protein purification, immobilization, and surface modifications (*12*−*14*). The hydrophobin membranes formed at interfaces can also have very special properties with respect to permeability (*15*) and can be useful for the attachment of cells and in tissue engineering (*16*−*19*).

Hydrophobins typically share quite a low sequence similarity at the protein level, but they always have one clearly distinguishing feature in their primary sequence, namely, eight Cys residues in a characteristic pattern. In this pattern, the third and fourth as well as the sixth and seventh Cys residues are always adjacent in the primary sequence. Using sequence alignments, the hydrophobins can be grouped into two classes, I and II (*1*, *20*). The work described here has been performed with the class II hydrophobins HFBI and HFBII of the fungus *Trichoderma reesei*. The most distinguishing difference in the properties between the two hydrophobin classes is probably the high tendency of class I members to self assemble into aggregates that have amyloid-like features (*21*−*24*). These aggregates are typically much more insoluble than the assemblies of the class II members. A comparison of protein properties and sequences of the class I and class II members suggests that there are significant differences between the two classes and that caution should be used when drawing conclusions about the function of one class on the basis of the results obtained for the other class.

The self-assembly of hydrophobins has received much attention. It has been shown that hydrophobins form films at the air−water interface. High-resolution atomic force microscopy has shown that these films can have a highly ordered structure with the protein molecules packed in an

† This work was funded by the National Graduate School in Informational and Structural Biology (GSz), the Academy of Finland (grant #205997), and Tekes.

* Corresponding author. Tel: +358 20722111. Fax: +358 207227071. E-mail: geza.szilvay@vtt.fi.

‡ VTT Biotechnology.

§ University of Helsinki.

10.1021/bi060620y CCC: $33.50
Published on Web 06/21/2006

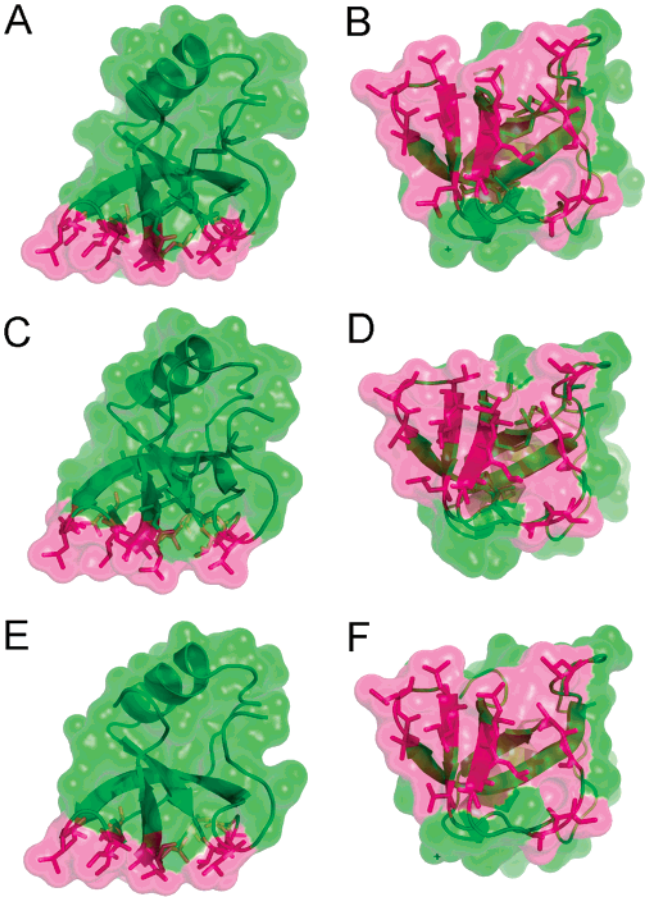

FIGURE 1: HFBI, NCys−HFBI, and HFBII have mesoscopic amphiphile structures. The conserved hydrophobic aliphatic amino acid residues form a planar hydrophobic patch (red) on one side of (A and B) HFBI, (C and D) NCys−HFBI and (E and F) HFBII. (B, D, and F) Bottom views of A, C, and E, respectively (*x*-axis rotated 90°). The *N*-terminal 18 amino acids of NCys−HFBI are not visible in the X-ray electron density map because of the high mobility of the long linker or protein degradation. The atomic coordinates for the images are obtained from X-ray crystal structures pdb ID 2FZ6 (HFBI), 2FZ7 (NCys−HFBI) (*49*), and 1R2M (HFBII) (*29*) (*47*). The Figures were produced with PyMOL (*48*).

ordered crystalline layer (*25*, *26*). Despite their high tendency to migrate to surfaces and interfaces, hydrophobins can show remarkable solubility. Dissolving the hydrophobin HFBI from *T. reesei* in water at a concentration of 100 mg/mL still produces a clear solution (*27*).

The lack of high-resolution structural data hampered the detailed study of hydrophobins for a long time. Using class I hydrophobins as models, it was suggested that hydrophobins exist as largely unstructured monomers in solution and attain their surface activity by conformational changes that occur when the protein encounters interfaces (*28*). A major breakthrough was achieved when the structure of HFBII from *T. reesei* was solved (*29*). On the basis of this structure, a general model for the function of hydrophobins could be envisioned. The X-ray structures of HFBI and its variant, NCys−HFBI (considered in this study), has been solved, showing that the structures are very similar to HFBII (Figure 1) (*49*). The structures of HFBII, HFBI, and NCys−HFBI show a core part consisting of a β-barrel structure with a stretch of α-helix on one side of the barrel. The whole structure is cross-linked by four disulfide bridges. On one face of the β-barrel, where two β-hairpin loops are exposed, a patch consisting solely of hydrophobic aliphatic side chains can be seen (Figure 1). These hydrophobic residues are highly conserved among class II hydrophobins and comprise half of all hydrophobic residues in the protein. The presence of the hydrophobic patch leads to two suggestions: (i) the hydrophobic patch makes the protein amphiphilic, and (ii) to compensate for the energetically unfavorable exposure of hydrophobic side chains at the surface, the protein must be highly stabilized by disulfide bridges. In this view, the protein can be described as a large, structurally rigid amphiphile. Apparently, the combination of these properties gives hydrophobins extraordinary properties as surfactants. It is interesting to note that there are attempts to produce synthetic molecules with similar architecture that also have properties such as adhesion and self-assembly (*30*).

A recent structural study of the class I hydrophobin EAS shows that EAS and HFBII share essentially the same core fold, the same disulfide bonding pattern, and the amphiphilic monomer architecture (*31*). Nevertheless, significant differences in the loop regions are evident.

The size and shape of the hydrophobic patch in the structure of the class II hydrophobins is likely to lead to some special functional consequences. Theoretical calculations show that hydrophobic cavities in water show a solvation free energy that is dependent on the size of the cavity. If a solute surface has a low curvature and an area of over 1 nm^2, it becomes impossible for water molecules to maintain hydrogen bonding around it (*32*). Thus, the solvation free energy is larger per unit surface area as the size of the continuous surface area increases. In the case of HFBI and HFBII, the flat hydrophobic patch is about 4 nm^2 and should be very effectively de-wetted. This geometrical feature is likely to contribute to the extraordinary surfactant properties of hydrophobins.

To understand how hydrophobins function as surfactants, it is of interest not only to study their behavior at interfaces, but also to know how they behave in bulk solution. Previous small-angle X-ray scattering (SAXS[1]) studies estimated the size of hydrophobin particles in a solution with high concentrations of HFBI and HFBII to correspond to tetramers, leading to the hypothesis that hydrophobins exist as tetramers in solution (*25*, *27*). However, very little information on the dynamics, concentration dependence, or the factors affecting hydrophobin intermolecular interactions could be obtained. In this work, our aim was to study the solution behavior of hydrophobins to see if they behave in a manner that is analogous to typical surfactants.

We chose Förster resonance energy transfer (FRET) (*33*) as the principal method for studying the interactions of hydrophobins in solution. This method provides an elegant way of studying the interactions between molecules in solution but requires the labeling of interacting molecules with a pair of fluorescent molecules. The fluorescent molecules are chosen so that the emission spectrum of one (the donor) overlaps the excitation spectrum of the other (the

[1] Abbreviations: CMC, critical micellization concentration; FRET, Förster resonance energy transfer; MALDI/TOF, matrix-assisted laser desorption ionization/time-of-flight; SAXS, small-angle X-ray scattering; SDS, sodium dodecylsulphate; SEC, size exclusion chromatography.

acceptor). If the acceptor and donor molecules are close enough, a transfer of energy will occur, and this transfer can be detected using a fluorescence spectrophotometer. For accurate experiments, we engineered the HFBI protein so that an extra Cys residue was added to its *N*-terminus. This allowed the site-specific and accurate labeling of HFBI by the chosen probes.

The data on the interactions of hydrophobins in solution supported a model where hydrophobins show a behavior analogous to that of typical surfactants, but the data also show that the behavior differs significantly in details.

MATERIALS AND METHODS

Site-Directed Mutagenesis and Production Strain. To get the best conditions for FRET measurements, we used a variant of HFBI that can be labeled at a specific position in the molecule. We designed a variant with an added single Cys residue at the *N*-terminal of the protein, NCys−HFBI. The *hfb1* gene was cut out from the plasmid pMQ121 (*34*) with *Bam*HI and *Sac*II (both from New England Biolabs) and ligated into the corresponding sticky end sites of pBluescript KS(−) (Stratagene, CA). The resulting plasmid, pGZ7, was transformed into the XL1-blue *Escherichia coli* strain. The QuikChange Site-Directed Mutagenesis kit (Stratagene, CA) was used according to the manufacturer's instructions to produce a variant *hfb1* gene with an insertion in the mature amino terminus after the signal sequence coding for SCPATTTGSSPGP resulting in plasmid pGZ9. The nucleotide oligos used were CCTCTCGAGG ACCGCAGCTG CCCCGCCACC ACCACCGGCT CCAGCCCTGG CCCTAGCAAC GGCAACGGC (sense) and GCCGTTGCCG TTGCTAGGGC CAGGGCTGGA GCCGGTGGTG GTGGCGGGGC AGCTGCGGTC CTCGAGAGG (antisense) (ordered from Sigma-Genosys Ltd.). The underlined sequence codes for the inserted amino acid sequence. However, the plasmid had a spontaneous mutation in the coding region, which was reverted with the QuikChange kit to yield the plasmid pGZ9AC. The modified *hfb1* insert was ligated as a *Bam*HI−*Sac*II fragment into pMQ121 to yield pGZ12. The expression cassette containing the modified *hfb1* under the control of *cbh1* regulatory sequences was released from pGZ12 using *Eco*RI and *Sph*I (New England Biolabs) and co-transformed with plasmid pToC202 (acetamide resistance) into the *T. reesei* Rut-C30 Δ*hfb2* strain VTT-D-99676 (*6*, *35*), essentially as described by Penttilä et al. (*36*). The formed Amd+ transformants were tested for high hydrophobin expression in shake flasks by slot blotting and Western analysis using HFBI-specific antibodies with standard protocols. The transformant selected for the NCys−HFBI production was named VTT D-061175.

Production and Purification of Hydrophobins. The *T. reesei* transformant VTT D-061175 was cultivated in a bioreactor for 94 h in media containing 40 g/L of lactose, 4.0 g/L of peptone, 1.0 g/L of yeast extract, 4.0 g/L of KH_2PO_4, 2.8 g/L of $(NH_4)SO_4$, 0.6 g/L of $MgSO_4 \cdot 7H_2O$, 0.8 g/L of $CaCl_2 \cdot 2H_2O$, and 2× trace elements. The bioreactor cultivations were performed without pH control to allow the culture medium pH to drop from 5 to 3 because the cultivations at pH 4−5 resulted in degraded NCys−HFBI as seen with matrix-assisted laser desorption ionization/time-of-flight (MALDI/TOF) mass spectroscopy (Institute of Biotechnology, University of Helsinki, Finland) (data not shown). The protein NCys−HFBI was purified from the biomass, essentially as described for HFBI by Linder et al. (*34*). Briefly, the biomass was treated with 4 mM guanidine hydrochloride in 200 mM Tris at pH 7.5 for 2 h. The supernatant was then diluted with water to double the volume. NCys−HFBI was extracted into an anionic surfactant (Berol 532, Akzo Nobel Surface Chemistry, Sweden) phase and back extracted into a fresh aqueous buffer with isobutanol. After reversed-phase chromatography, the peak containing NCys−HFBI was lyophilized. Mass spectroscopy (MALDI/TOF) analysis showed a 2-fold mass presumably due to the oxidation of the introduced cysteine sulfhydryls resulting in a disulfide-linked hydrophobin dimer. Wild-type HFBI and HFBII were produced as previously described (*34*).

Conjugation. Before chemical conjugation, the disulfide forming the NCys−HFBI dimer (see above) was selectively reduced with 50 mM dithiothreitol (Sigma-Aldrich Chemie GmbH, Germany) in 50 mM acetate buffer at pH 5 for 1 h at 37 °C. The NCys−HFBI was then purified from the reaction mixture with reversed-phase chromatography and, concomitantly, concentrated by solvent evaporation. MALDI/TOF analysis and functional studies showed that only the additional Cys residue was reduced under these conditions, and the internal disulfides remained intact. The total reduction of the protein requires reducing conditions at high temperatures (data not shown). The reduced NCys−HFBI was conjugated with Cy3-monomaleimide or Cy5-monomaleimide (GE Healthcare) according to the manufacturer's instructions. The separation of nonreacted dye molecules was achieved with reversed-phase chromatography, and the eluted labeled NCys−HFBI was concentrated with vacuum centrifugation and stored in the dark at 4 °C.

MALDI/TOF analysis showed that the labeling was successful because the major peak corresponded to the labeled protein. The degree of labeling was determined by dividing the concentration of incorporated dye by that of the protein. The extinction coefficients used for determining the dye concentrations were 150 000 $M^{-1} \cdot cm^{-1}$ (at 549 nm) and 250 000 $M^{-1} \cdot cm^{-1}$ (at 647 nm) for Cy3−NCys−HFBI and Cy5−NCys−HFBI, respectively. Absorption spectra were collected with a Cary 100 spectrophotometer (Varian, Inc., CA). The protein concentration was determined with quantitative amino acid analysis (Amino acid analysis laboratory, Uppsala University, Sweden).

FRET Measurements of Fluorophore Conjugated Hydrophobins. Stock solutions of 18.5 μM total hydrophobin concentration in 50 mM Na-acetate buffer at pH 5.0 were diluted for FRET measurements. In the donor−acceptor stock solution, the concentration of Cy3−NCys−HFBI and Cy5−NCys−HFBI was 9.2 μM each. In donor or acceptor only stock solutions, 9.2 μM HFBI was included to replace the excluded acceptor or donor partner. For studying the interactions with other compounds, the stock solutions were diluted into the respective compound-containing solution to yield a 2.1 μM total labeled hydrophobin concentration.

The fluorescence spectra of the diluted samples were collected with a steady-state fluorescence spectrophotometer Cary Eclipse (Varian, Inc., CA) at 22 °C unless otherwise stated. The efficiency of energy transfer, *E*, was calculated using the enhanced fluorescence of the acceptor fluorophore as described by Clegg (*37*). The samples were excited at

516 nm (donor excitation) while recording the emission spectra of both the donor and acceptor. The acceptor spectrum was extracted by subtracting a normalized donor-only spectrum from the measured donor−acceptor spectrum. The resulting spectrum contained the directly excited acceptor emission and the acceptor emission due to FRET. This spectrum was divided by the fluorescence of the same sample excited at 605 nm, where only the acceptor is excited. The resulting spectrum, $(\text{ratio})_A$ is dependent on FRET E and can be described as follows:

$$(ratio)_A = \left(Ed^+ \frac{\epsilon^D(516)}{\epsilon^A(605)} + \frac{\epsilon^A(516)}{\epsilon^A(605)} \right) \cdot \frac{\phi^A(\nu_1)}{\phi^A(\nu_2)} \qquad (1)$$

where $\epsilon(\lambda)$ denotes the extinction coefficient at wavelength λ, and the superscripts denote donor (D) and acceptor (A) (*37*). The donor labeling degree is marked as d^+. This term also includes any incorporation of the nonlabeled HFBI to the samples, that is, the labeling degree reduction. The ratio of the acceptor quantum yields $\varphi^A(\nu_i)$ at FRET measurement wavelength (ν_1) and acceptor emission wavelength (ν_2) is unity because ν_1 was equal to ν_2 in all experiments. $\epsilon^D(516)/\epsilon^A(605)$ was determined to be 1.116 and $\epsilon^A(516)/\epsilon^A(605)$ 0.0287.

For temperature scans, a water thermostated (C25P, Thermo Haake) cell holder was used. The heating rate was 1.67 °C/min and the cooling rate approximately 0.65 °C/min. The sample temperature was measured with a temperature probe inserted into the cuvette. The general effect of fluorescence decrease due to heating is taken into account in FRET because the FRET E was determined through the relative increase of acceptor fluorescence as described above.

Size Exclusion Chromatography. Hydrophobin samples with varying concentrations were injected (100 μL) into a Superdex 75 column (Amersham, Sweden) and eluted with 50 mM Na-acetate buffer at pH 5.0 containing 0.2 M NaCl using an Äkta Explorer (Amersham, Sweden) chromatography system. Sample elution was detected with UV absorbance at 230 nm. Reference samples were used to determine a standard line for molecular size determination. The references used were vitamin B-12 (1.4 kDa, Sigma), aprotinin (6.5 kDa, Sigma), ribonuclease A (13.7 kDa, Amersham Pharmacia Biotech, Sweden), and ovalbumin (43.0 kDa, Amersham Pharmacia Biotech, Sweden).

RESULTS

FRET between Hydrophobin Monomers. The association of fluorescent-labeled NCys−HFBI proteins in solution was studied with FRET. Because FRET is strongly distance-dependent, it provides a convenient way to study the changes in the multimeric states of associating molecules (*33*). The sensitized emission of the acceptor (Cy5−NCys−HFBI) was measured while exciting the donor (Cy3−NCys−HFBI) at 516 nm. The fluorescence spectra of the donor-labeled hydrophobin, acceptor-labeled hydrophobin, and an equimolar mixture of donor and acceptor are shown in Figure 2. The introduction of the acceptor to a donor sample decreases the measured donor fluorescence emission and increases the acceptor emission.

The energy transfer in donor−acceptor samples was calculated from the ratio of the true sensitized acceptor emission at 665 nm and the fluorescence of the directly excited acceptor as described in Materials and Methods. The advantage of the method developed by Clegg (*37*) is that only the shape of the donor-only control sample spectrum is used. Therefore, uncontrolled small changes in protein concentration, due to the intrinsic property of hydrophobins to adsorb to surfaces, do not affect data reproducibility.

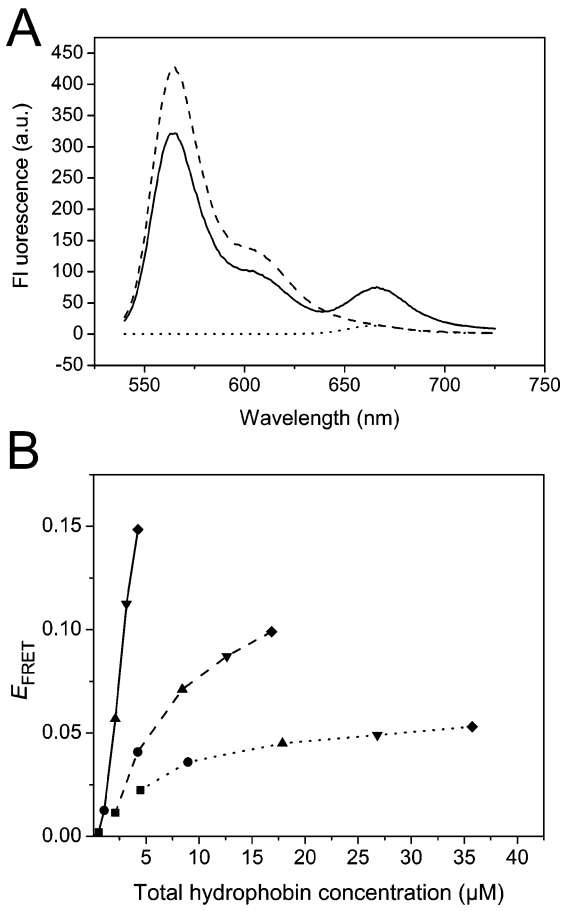

FIGURE 2: (A) Emission spectra of FRET samples at 4.2 μM total protein concentration. Samples with equimolar amounts of Cy3−NCys−HFBI and Cy5−NCysHFBI (___), Cy3−NCys−HFBI and HFBI (----), and Cy5−NCys−HFBI and HFBI (.....). (B) Concentration dependence of energy transfer between fluorescent-labeled hydrophobins. Uncorrected FRET values of samples with total labeled concentrations of 0.5 μM (■), 1.1 μM (●), 2.1 μM (▲), 3.2 μM (▼), and 4.2 μM (♦). Ratio of labeled hydrophobin/nonlabeled HFBI was 1:0 (___), 1:3.0 (----), and 1:7.5 (.....).

FRET was determined at different hydrophobin concentrations in thermodynamic equilibrium studies. After sample preparation (approximately 2 min), no change in FRET was observed within 90 min. First, we measured FRET in samples where half of the hydrophobins were donor-labeled and half were acceptor-labeled. FRET increased almost linearly as a function of hydrophobin total concentration up to 5 μM (solid line, Figure 2B), which was at the limit of the linear range of the fluorophore intensities.

To study the behavior of HFBI at higher protein concentrations, the labeled sample was mixed with nonlabeled HFBI. Labeled NCys−HFBI and nonlabeled HFBI protein were mixed at the following ratios: 1:3.0 and 1:7.5 (Figure 2B). We noted that the addition of nonlabeled HFBI to a given concentration of FRET-pair labeled-HFBI influenced the FRET efficiency in two counteractive ways. On the one hand, FRET efficiency decreased because HFBI replaced the

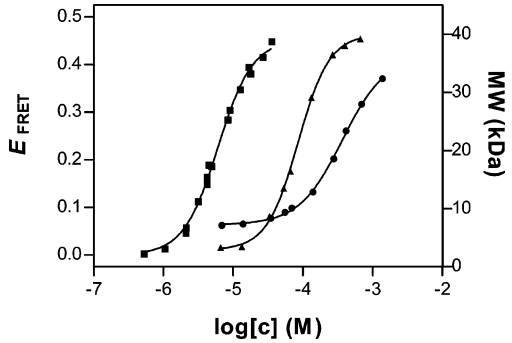

FIGURE 3: Concentration dependence of hydrophobin multimerization. HFBI (▲) and HFBII (●) were analyzed with SEC (right *y*-axis) and labeled NCys−HFBI (■) with FRET (left *y*-axis). The protein samples with the indicated concentrations were injected into the SEC column, and the molecular mass of the complexes were determined from the elution volume. True sample concentrations in the SEC results deviate from the indicated concentrations because sample dilution during the chromatography run is not taken into account.

labeled hydrophobins in the multimers and, hence, decreased the number of donor−acceptor pairs. On the other hand, FRET efficiency increased, especially at low initial concentrations, because the increase in total hydrophobin concentration pushed the equilibrium toward association (FRET pair formation). At low total concentration, the effect of concentration increase outbalances the effect of HFBI competition. At higher concentrations, where multimerization is approaching the maximum, only the effect of nonlabeled HFBI competition is present.

The FRET efficiency was corrected for nonlabeled HFBI incorporation by considering the HFBI addition as a reduction in the labeling degree as described in Materials and Methods. These data were then plotted in a separate graph (Figure 3, squares). The effect of decreasing the fraction of labeled HFBI caused a linear effect in the FRET efficiency. In Figure 3 (squares), this can be noted by the overlapping of the curves from Figure 2B with different labeling degrees. This shows that labeling had no effect on the function of NCys−HFBI and that the NCys−HFBI and wild-type have identical behavior in solution. At hydrophobin concentrations around 20 μM, the FRET *E* approached a maximum value. The concentration producing 50% of the maximum response (EC_{50}) was determined to be 6.1 ±0.3 μM, and a Hill slope of 1.8 ±0.1 was obtained by fitting a sigmoidal dose−response curve to the data (Figure 3, squares) using GraphPad Prism version 3.00 for Windows (GraphPad Software, San Diego CA, www.graphpad.com).

Interaction of the Cys-Conjugated Hydrophobins in the Presence of Cosolutes. FRET measurements were used for determining changes in association in different conditions and to see how the homologous hydrophobin HFBII from *T. reesei* could interact with HFBI. As described in the previous section, the addition of nonlabeled HFBI to a donor−acceptor NCys−HFBI pair increases or decreases FRET *E* depending on the multimeric state of the labeled NCys−HFBI. The addition of 12 and 30 μM HFBI to 3.2 μM labeled NCys−HFBI decreased FRET *E* to 81.0% and 45.6%, respectively. However, HFBII additions of the same concentrations had a smaller effect, changing FRET *E* to 102.2% and 75.6%, respectively (Figure 4). Experiments performed at lower concentrations did not show the effect

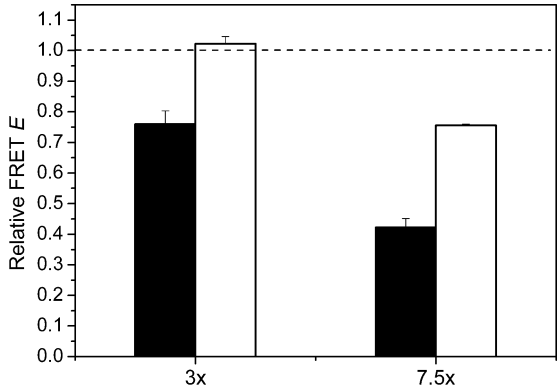

FIGURE 4: HFBII interaction with fluorescent-labeled NCys−HFBI. FRET *E* was measured from samples of total labeled NCys−HFBI concentration of 3.2 μM. Indicated amounts of excess HFBI (black columns) or HFBII (white columns) were added to the sample. Results are means, and error bars indicate standard deviations ($n = 3$).

Table 1. Comparison of the Effects of Detergents, Ethanol, and Salts on NCys−HFBI Association

cosolute	FRET *E* signal compared to the control (%)[a]
0.1% Tween-20	97.0 ± 0.4
0.1% SDS[b]	24.8 ± 1.2
10% ethanol	41.9 ± 1.5
25% ethanol	6.5 ± 1.8
50% ethanol	1.5 ± 1.0
0.5 M $(NH_4)_2SO_4$	430.8 ± 13.5
0.5 M NaCl	195.9 ± 7.9

[a] The FRET efficiency upon cosolute addition at 2.1 μM total hydrophobin concentration in 50 mM Na-acetate buffer at pH 5.0 compared to that of samples without added cosolutes. [b] SDS, sodium dodecyl sulfate. The results are the mean ± standard deviation ($n = 3$).

of added HFBII as clearly because of the counter effective effects of competition and dilution, which were more pronounced at these concentrations.

The FRET method also makes it possibile to study which external factors affect the association of hydrophobins. Energy transfer between hydrophobin monomers in the presence of sodium dodecyl sulfate (SDS), Tween-20, ethanol, or the cellulase enzyme CBHI is summarized in Table 1. SDS and ethanol decreased energy transfer very efficiently, whereas 0.1% Tween-20 and 1.5 μM CBHI had a much smaller effect. The salts NaCl and $(NH_4)_2SO_4$ at 0.5 M clearly increased FRET *E*.

The energy transfer efficiency was observed to be dependent on temperature (Figure 5). A reversible FRET increase was observed when the sample was heated from 11 to 56 °C. Further heating to 84 °C caused a decrease in FRET *E*, which was also largely reversible.

Size Exclusion Chromatography. Size exclusion chromatography (SEC) was used as a supporting method for studying hydrophobin multimer formation. The multimer size at different concentrations for HFBI and HFBII was determined (Figure 3; triangles and circles, respectively). Skew peaks were observed for HFBI when the injected sample had a concentration below 65 μM. HFBII eluted as multiple peaks when the injected sample concentration was above 140 μM; therefore, the most populated peak (highest absorbance),

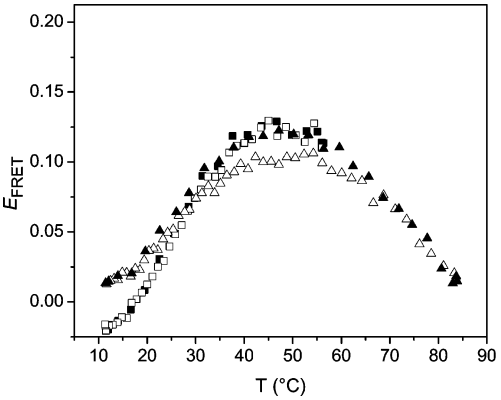

FIGURE 5: Temperature scans of energy transfer measurements. A 2.1 μM donor−acceptor labeled sample was heated (black symbols) followed by cooling (white symbols). Heating temperatures were 11−56 °C (■, □) and 11−84 °C (▲, △).

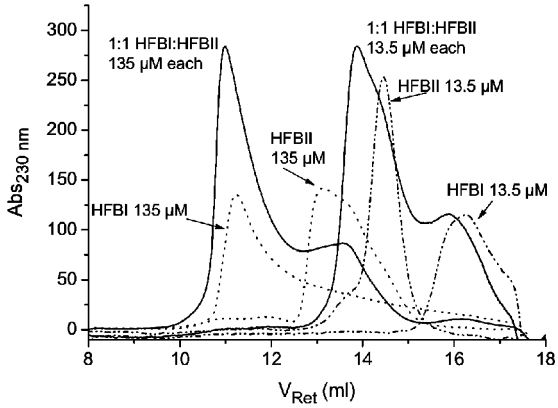

FIGURE 6: HFBI−HFBII heteromultimerization studied with SEC. Equimolar mixtures of HFBI and HFBII (___) were injected into a SEC column and segregated, or coelution was determined. Pure HFBI or HFBII was injected at 135 μM (.....) and 13.5 μM (-•-•-). The curves for the low concentration samples were multiplied by 11 to help with the comparison to the high concentration samples.

which also always eluted corresponding to the highest mass, was used for the plot in Figure 3. In addition, a small peak (less than 0.2% of the total peak area) eluting in the void volume of the chromatography column of HFBI and HFBII samples at higher concentrations was observed, corresponding to particles over about 100 kDa in size. These large particles may be small amounts of protein aggregates in the HFBI and HFBII samples.

A sigmoidal dose−response curve was fitted to the data, and the Hill slope was calculated from the fit using GraphPad Prism version 3.00 for Windows. The calculated maximum multimer sizes for HFBI and HFBII were 40.0 ± 0.5 and 36 ± 1 kDa, respectively. The monomer molecular weights of HFBI and HFBII are 7532.5 and 7188.3, respectively. EC_{50} values for HFBI and HFBII were 85 ± 2 and 367 ± 19 μM, respectively. The obtained Hill slope for HFBI was 1.9 ± 0.1 and 1.4 ± 0.1 for HFBII, indicating positive cooperativity.

The data indicated that homotetramerization of HFBI and HFBII was cooperative. A Hill slope value of 1.9 and 1.8 was obtained for HFBI with SEC and FRET, respectively, and 1.4 for HFBII (SEC). The definition for cooperativity is that the binding of subsequent molecules depend on the binding of the preceding molecules. The dimerization of dimers inherently depends on the formation of dimers, that is, tetramers can form only if dimers are present; hence, there is always cooperativity in this type of tetramerization.

Equimolar mixtures of HFBI and HFBII were analyzed with SEC (Figure 6). At the total protein concentration of 27 μM, two separate peaks eluted at volumes closely corresponding to the single proteins at their respective concentrations. When the total concentration was increased to 270 μM, partial coelution was observed as seen in the increase of the HFBI peak (higher mass) and a decrease in the HFBII peak. This was verified by western blotting (data not shown).

DISCUSSION

We were successful in finding a suitable pair of fluorescent molecules that allowed the study of the interactions between HFBI molecules in solution. The FRET signal from a mixture of Cy3- and Cy5-labeled HFBI was highly dependent on the total HFBI concentration (Figure 3). A maximum level of FRET efficiency was obtained at about 20 μM concentration of protein, and the EC_{50} was 6 μM. For comparison, it has been shown that the water surface tension is reduced with increasing HFBI concentration until about 7 μM, and above that concentration, no significant surface tension reduction is observed (*38*). This indicates that at the concentration where the systems interfaces are fully occupied and the addition of hydrophobins does not reduce the water surface tension further, hydrophobins start to associate into multimers in solution. Our data show that HFBI associates in solution in a concentration-dependent manner, suggesting a behavior similar to the general behavior of surfactants in solution. That is, the hydrophobic parts are excluded from contact with water by the formation of a multimer in a concentration-dependent manner. The formation of complexes where the hydrophobic patches are likely to be shielded explains many of the properties of HFBI, such as its high solubility in water. The kinetics of association and dissociation of the multimers was faster than was possible to measure with a conventional spectrophotometer, that is, equilibrium was established within seconds.

The FRET data gave accurate values for the concentration dependency of the association in solution but did not directly reveal the nature or the size of the complexes formed in solution. The nature of the complexes were, therefore, studied by SEC. Using SEC, it is possible to obtain information about the size of the molecular aggregates, but because the sample was diluted and constantly changing during the chromatographic run, the exact concentration of the protein during the run is not known. HFBI samples of different concentration were injected, and the retention time of the eluant peak was followed as a function of concentration. In Figure 3 (triangles), the corresponding molecular weight (calculated from the retention time) is plotted as a function of the concentration of the injected sample. The real concentrations of protein in the eluted peaks were much lower. When high concentrations of protein were injected, the peak eluted at retention times corresponding to a tetramer of the protein and at low concentrations; the elution corresponded either to a dimer or a monomer. We have previously studied solutions of HFBI and HFBII using SAXS at high concentration (10 g/L, 1.3 mM) (*27*). It was found that the protein particles were well defined and had a size corresponding to tetramers. However, lower protein concentrations could not

be analyzed using SAXS because of the loss of scattering intensity on sample dilution. The plots of the independent FRET and SEC data show a practically identical shape for HFBI. The combined information strongly suggests that HFBI will combine to form tetramers in solution so that all HFBI exists as tetramers at concentrations above 20 μM. The shape of the curve suggests a cooperative association process. It is likely that the process involves combination of monomers to dimers with the successive combination of dimers to tetramers. Powers et al. (*39*) have shown that the mechanism of tetramerization via dimers is evolutionally favored over tetramerization via dimers and trimers. The exact portion of each hydrophobin multimeric component cannot be calculated from our data. Dimers were found as the crystallographic unit cell in the structure determination of HFBII (*29*). In the recent structure determination of HFBI, tetrameric packing was observed (*49*). In addition, the class I hydrophobin SC3 has also been reported to associate in solution to dimers and tetramers (*40*).

We have previously determined the dissociation constant of a HFBI−endoglucanase I core enzyme fusion protein (HFBI−EGIc) for hydrophobic silanized glass to be 0.44 μM (*12*). Competition experiments showed that the affinity of free HFBI is very similar. Comparing with the current FRET data, it seems that the affinity of a monomer for a multimer is approximately 1 order of magnitude lower than its affinity for surfaces. This is in good agreement with our model (*29*), where hydrophobin multimerization was suggested to protect the hydrophobic parts and that these associations disassemble at the interface to form monolayers. According to this model, the protein−protein affinity in the solution multimers needs to be lower than the protein−interface affinity. Detergents, for example, function in a similar manner. Below their critical micellization concentration (CMC), detergents occupy interfaces, whereas micelles are formed above the CMC.

Our conclusion is that hydrophobins do not form micelle-like structures in the same way as detergents do. Instead, they form defined tetramers and dimers that function in way that is analogous to micelle formation. Next, we asked the question whether the formation of multimers is a specific process that involves molecular recognition or if it, to some extent, involves a nonspecific association, where the hydrophobic parts are shielded without the involvement of specific protein−protein structural interactions. That is, if two different hydrophobins are mixed in the same solution, then will each form homomultimers separately, containing one type of hydrophobin, or will heteromultimers form containing a mixture of both types of protein? This question is of relevance for fungal biology, for example, because it is not known why several hydrophobin genes are typically found in the same organism and if the different hydrophobins interact or have different roles.

We used both FRET and SEC to study the interaction between HFBI and HFBII. Loading different concentrations of HFBII on the size exclusion column gave results similar to that for HFBI, namely, the retention time increased (smaller molecular weight) with lower concentrations (Figure 3, spheres). However, the retention times were different from those of HFBI, showing that the tendency to form multimers is similar but not the same. Next, we loaded mixtures of HFBI and HFBII onto the column. At low concentrations, the two proteins eluted as if they had been injected as pure samples, indicating that they do not form mixed multimers. However, at high concentrations, there was a noticeable increase in the area of the fast-eluting peak. We also noted that HFBII could not decrease the FRET *E* of NCys−HFBI as efficiently as the nonlabeled HFBI. It is possible that weak nonspecific interactions are involved in the HFBI−HFBII heteromultimers. However, because of the almost identical hydrophobic patches and the relatively high sequence identity (63%) between HFBI and HFBII (*41*, *42*), more specific interactions may be involved. We suggest that the interactions at low concentrations, probably involving dimer formation, are not affected by the presence of another type of hydrophobin and that the interaction is specific to a certain hydrophobin. The FRET and SEC data support the conclusion that at higher concentrations where it is likely that tetramer formation dominates there seems to be an interaction between the different proteins. According to this interpretation, the interactions involved in dimer formation are different from those leading to tetramer formation. In a system where tetramerization is formed by the dimerization of dimers, two different subunit interactions (and affinities) need to be present. It remains to be seen whether it is a general phenomenon that the interaction is preferentially with only hydrophobins of the same type.

To learn more about the interactions between individual hydrophobin molecules, the factors leading to a change of FRET at constant protein concentrations were investigated. Ethanol is known to dissolve some of the aggregates that class II hydrophobins form. Supporting these data, we found a clear loss of signal with increasing ethanol concentration. Similarly, SDS also efficiently reduced the FRET signal (Table 1). Surprisingly, the nonionic surfactant Tween-20 did not cause any change in the signal. No effect in the FRET signal was found when the possibility of interactions between other proteins and hydrophobins was investigated by the addition of the cellulase enzyme CBHI. We used CBHI because it is the major secreted protein from *T. reesei* and is produced in large amounts. The salts NaCl and $(NH_4)_2SO_4$ strongly increased FRET *E*, NaCl being less effective on a molar basis. We can conclude that solvents such as ethanol move the equilibrium toward monomers and salts in high concentrations toward multimerization. In a previous work, we used SDS to remove hydrophobin from the mycelium to purify hydrophobins (*34*, *43*), and therefore, the decreased associations between HFBI when mixed with SDS were expected. Our previous experience with HFBI shows that SDS does not irreversibly alter either its structure or its function (*34*).

The temperature dependency of the FRET showed an increase in association up to about 45 °C and a decrease when the temperature was further increased (Figure 5). HFBI itself has been found to be very temperature stable, with no change in the circular dichroism spectrum even when heated to 90 °C (*38*). Our interpretation is, therefore, that the temperature dependent change in FRET is due to a change in the multimerization state and is not the result of thermal protein denaturation. The reversibility of the effect also indicates that protein denaturation does not occur. This general temperature dependency of HFBI association is in line with what is expected for the temperature dependency of the hydrophobic effect. The hydrophobic effect should

show an increase going from low to medium temperatures and a decrease again from medium to high temperatures (*44*−*46*). We, therefore, expect that association would be driven mostly by hydrophobic interactions. The effects of added salts or solvents (Table 1) are also completely in line with the conclusion that hydrophobic interactions are a driving force in hydrophobin multimerization.

In previous studies, it has been shown that hydrophobins readily self assemble to various higher-order structures. In the case of class I hydrophobins, the amyloid -like rodlet layer is a characteristic feature (*4*). In the case of HFBI, HFBII, and class II hydrophobins in general, various needle-like crystals and structured surface films have been observed (*25*, *27*). These assemblies do not typically form spontaneously from protein in solution but require some sort of external triggering, such as shaking, passing bubbles through the sample, or drying the sample. In the surface films, it was observed that the basic repeating unit had a size corresponding to a protein tetramer (*25*). The corresponding observation was made for crystalline assemblies of HFBII (*27*). In this work, we showed that tetramers are spontaneously formed in solution, but it remains unclear as to how tetramer formation in solution is connected to the tetramer-sized units in surface films, for example. It is unlikely that they are the same because in solution, the hydrophobic areas must be shielded within the complex, and on the air−water interface, the hydrophobic part must be exposed to the air. Nonetheless, it remains a possibility that solution tetramerization is a step or a nucleation event toward the formation of higher-order assemblies.

The current work supports the picture that HFBI and related hydrophobins behave like surfactants in general but that they have unique features that give them properties that have not been seen previously in any surfactant system. Very little has been known about their behavior in solution. The two perhaps most important findings here are that, first, defined complexes are formed in a way analogous to micelle formation by traditional surfactants and, second, these micelle-like complexes involve specific molecular interactions so that different types of hydrophobins do not preferentially interact.

ACKNOWLEDGMENT

We gratefully acknowledge Harry Boer for his comments on the manuscript. We thank Michael Bailey for help with the bioreactor cultivations and Riitta Suihkonen for excellent technical assistance.

REFERENCES

1. Linder, M. B., Szilvay, G. R., Nakari-Setälä, T., and Penttilä, M. E. (2005) Hydrophobins: the protein amphiphiles of fungi, *FEMS Microbiol. Rev. 29*, 877−896.
2. Wösten, H. A., and de Vocht, M. L. (2000) Hydrophobins, the fungal coat unravelled, *Biochim. Biophys. Acta 1469*, 79−86.
3. Wessels, J. G., de Vries, O. M., Ásgeirsdóttir, S. A., and Springer, J. (1991) The thn mutation of *Schizophyllum commune*, which suppresses formation of aerial hyphae, affects expression of the Sc3 hydrophobin gene, *J. Gen. Microbiol. 137*, 2439−2445.
4. Wösten, H. A., Ásgeirsdóttir, S. A., Krook, J. H., Drenth, J. H., and Wessels, J. G. (1994) The fungal hydrophobin Sc3p self-assembles at the surface of aerial hyphae as a protein membrane constituting the hydrophobic rodlet layer, *Eur. J. Cell Biol. 63*, 122−129.
5. Talbot, N. J. (1999) Fungal biology. Coming up for air and sporulation, *Nature 398*, 295−296.
6. Askolin, S., Penttilä, M., Wösten, H. A., and Nakari-Setälä, T. (2005) The *Trichoderma reesei* hydrophobin genes hfb1 and hfb2 have diverse functions in fungal development, *FEMS Microbiol. Lett. 253*, 281−288.
7. Kershaw, M. J., Thornton, C. R., Wakley, G. E., and Talbot, N. J. (2005) Four conserved intramolecular disulphide linkages are required for secretion and cell wall localization of a hydrophobin during fungal morphogenesis, *Mol. Microbiol. 56*, 117−125.
8. Talbot, N. J., Kershaw, M. J., Wakley, G. E., de Vries, O., Wessels, J., and Hamer, J. E. (1996) MPG1 Encodes a fungal hydrophobin involved in surface interactions during infection-related development of *Magnaporthe grisea*, *Plant Cell 8*, 985−999.
9. Talbot, N. J., Ebbole, D. J., and Hamer, J. E. (1993) Identification and characterization of MPG1, a gene involved in pathogenicity from the rice blast fungus *Magnaporthe grisea*, *Plant Cell 5*, 1575−1590.
10. Wösten, H. A. B. (2001) Hydrophobins: multipurpose proteins, *Annu. Rev. Microbiol. 55*, 625−646.
11. Wösten, H. A., van Wetter, M. A., Lugones, L. G., van der Mei, H. C., Busscher, H. J., and Wessels, J. G. (1999) How a fungus escapes the water to grow into the air, *Curr. Biol. 9*, 85−88.
12. Linder, M., Szilvay, G. R., Nakari-Setälä, T., Söderlund, H., and Penttilä, M. (2002) Surface adhesion of fusion proteins containing the hydrophobins HFBI and HFBII from *Trichoderma reesei*, *Protein Sci. 11*, 2257−2266.
13. Linder, M. B., Qiao, M., Laumen, F., Selber, K., Hyytiä, T., Nakari-Setälä, T., and Penttilä, M. E. (2004) Efficient purification of recombinant proteins using hydrophobins as tags in surfactant-based two-phase systems, *Biochemistry 43*, 11873−11882.
14. Nakari-Setälä, T., Azeredo, J., Henriques, M., Oliveira, R., Teixeira, J., Linder, M., and Penttilä, M. (2002) Expression of a fungal hydrophobin in the *Saccharomyces cerevisiae* cell wall: effect on cell surface properties and immobilization, *Appl. Environ. Microbiol. 68*, 3385−3391.
15. Wang, X., Shi, F., Wösten, H. A. B., Hektor, H., Poolman, B., and Robillard, G. T. (2005) The SC3 hydrophobin self-assembles into a membrane with distinct mass transfer properties, *Biophys. J. 88*, 3434−3443.
16. Janssen, M. I., van Leeuwen, M. B., Scholtmeijer, K., van Kooten, T. G., Dijkhuizen, L., and Wösten, H. A. (2002) Coating with genetic engineered hydrophobin promotes growth of fibroblasts on a hydrophobic solid, *Biomaterials 23*, 4847−4854.
17. Janssen, M. I., van Leeuwen, M. B., van Kooten, T. G., de Vries, J., Dijkhuizen, L., and Wösten, H. A. (2004) Promotion of fibroblast activity by coating with hydrophobins in the beta-sheet end state, *Biomaterials 25*, 2731−2739.
18. Scholtmeijer, K., Janssen, M. I., Gerssen, B., de Vocht, M. L., van Leeuwen, B. M., van Kooten, T. G., Wösten, H. A., and Wessels, J. G. (2002) Surface modifications created by using engineered hydrophobins, *Appl. Environ. Microbiol. 68*, 1367−1373.
19. Scholtmeijer, K., Wessels, J. G., and Wösten, H. A. (2001) Fungal hydrophobins in medical and technical applications, *Appl. Microbiol. Biotechnol. 56*, 1−8.
20. Wessels, J. G. H. (1994) Developmental regulation of fungal cell wall formation, *Annu. Rev. Phytopathol. 32*, 413−437.
21. Wösten, H. A. B., de Vries, O. M. H., and Wessels, J. G. H. (1993) Interfacial self-assembly of a fungal hydrophobin into a hydrophobic rodlet layer, *Plant Cell 5*, 1567−1574.
22. Butko, P., Buford, J. P., Goodwin, J. S., Stroud, P. A., McCormick, C. L., and Cannon, G. C. (2001) Spectroscopic evidence for amyloid-like interfacial self-assembly of hydrophobin Sc3, *Biochem. Biophys. Res. Commun. 280*, 212−215.
23. de Vocht, M. L., Reviakine, I., Wosten, H. A., Brisson, A., Wessels, J. G., and Robillard, G. T. (2000) Structural and functional role of the disulfide bridges in the hydrophobin SC3, *J. Biol. Chem. 275*, 28428−28432.
24. Mackay, J. P., Matthews, J. M., Winefield, R. D., Mackay, L. G., Haverkamp, R. G., and Templeton, M. D. (2001) The hydrophobin EAS is largely unstructured in solution and functions by forming amyloid-like structures, *Structure 9*, 83−91.
25. Paananen, A., Vuorimaa, E., Torkkeli, M., Penttilä, M., Kauranen, M., Ikkala, O., Lemmetyinen, H., Serimaa, R., and Linder, M. B. (2003) Structural hierarchy in molecular films of two class II hydrophobins, *Biochemistry 42*, 5253−5258.

26. Kisko, K., Torkkeli, M., Vuorimaa, E., Lemmetyinen, H., Seeck, O. H., Linder, M., and Serimaa, R. (2005) Langmuir−Blodgett films of hydrophobins HFBI and HFBII, *Surf. Sci. 584*, 35−40.
27. Torkkeli, M., Serimaa, R., Ikkala, O., and Linder, M. (2002) Aggregation and self-assembly of hydrophobins from *Trichoderma reesei*: low resolution structural models, *Biophys. J. 83*, 2240−2247.
28. Zangi, R., de Vocht, M. L., Robillard, G. T., and Mark, A. E. (2002) Molecular dynamics study of the folding of hydrophobin SC3 at a hydrophilic/hydrophobic interface, *Biophys. J. 83*, 112−124.
29. Hakanpää, J., Paananen, A., Askolin, S., Nakari-Setälä, T., Parkkinen, T., Penttilä, M., Linder, M. B., and Rouvinen, J. (2004) Atomic resolution structure of the HFBII hydrophobin, a self-assembling amphiphile, *J. Biol. Chem. 279*, 534−539.
30. Stupp, S. I., LeBonheur, V. V., Walker, K., Li, L. S., Huggins, K. E., Keser, M., and Amstutz, A. (1997) Supramolecular materials: self-organized nanostructures, *Science 276*, 384−389.
31. Kwan, A. H., Winefield, R. D., Sunde, M., Matthews, J. M., Haverkamp, R. G., Templeton, M. D., and Mackay, J. P. (2006) Structural basis for rodlet assembly in fungal hydrophobins, *Proc. Natl. Acad. Sci. U.S.A. 103*, 3621−3626.
32. Chandler, D. (2005) Interfaces and the driving force of hydrophobic assembly, *Nature 437*, 640−647.
33. Lakowicz, J. R. (1999) *Principles of Fluorescence Spectroscopy*, 2nd ed., Kluwer Academic/Plenum Publishers, New York.
34. Linder, M., Selber, K., Nakari-Setälä, T., Qiao, M., Kula, M.-R., and Penttilä, M. (2001) The hydrophobins HFBI and HFBII from *Trichoderma reesei* showing efficient interactions with nonionic surfactants in aqueous two-phase systems, *Biomacromolecules 2*, 511−517.
35. Bailey, M., Askolin, S., Hörhammer, N., Tenkanen, M., Linder, M., Penttilä, M., and Nakari-Setälä, T. (2002) Process technological effects of deletion and amplification of hydrophobins I and II in transformants of *Trichoderma reesei*, *Appl. Microbiol. Biotechnol. 58*, 721−727.
36. Penttilä, M., Nevalainen, H., Rättö, M., Salminen, E., and Knowles, J. (1987) A versatile transformation system for the cellulolytic filamentous fungus *Trichoderma reesei*, *Gene 61*, 155−164.
37. Clegg, R. M. (1992) Fluorescence resonance energy transfer and nucleic acids, *Methods Enzymol. 211*, 353−388.
38. Askolin, S., Linder, M., Scholtmeijer, K., Tenkanen, M., Penttilä, M., de Vocht, M. L., and Wösten, H. A. (2006) Interaction and comparison of a class I hydrophobin from *Schizophyllum commune* and class II hydrophobins from *Trichoderma reesei*, *Biomacromolecules 7*, 1295−1301.
39. Powers, E. T., and Powers, D. L. (2003) A perspective on mechanisms of protein tetramer formation, *Biophys. J. 85*, 3587−3599.
40. Wang, X., Graveland-Bikker, J. F., de Kruif, C. G., and Robillard, G. T. (2004) Oligomerization of hydrophobin SC3 in solution: from soluble state to self-assembly, *Protein Sci. 13*, 810−821.
41. Nakari-Setälä, T., Aro, N., Kalkkinen, N., Alatalo, E., and Penttilä, M. (1996) Genetic and biochemical characterization of the *Trichoderma reesei* hydrophobin HFBI, *Eur. J. Biochem. 235*, 248−255.
42. Nakari-Setälä, T., Aro, N., Ilmén, M., Muñoz, G., Kalkkinen, N., and Penttilä, M. (1997) Differential expression of the vegetative and spore-bound hydrophobins of *Trichoderma reesei* − cloning and characterization of the *hfb2* gene, *Eur. J. Biochem. 248*, 415−423.
43. Askolin, S., Nakari-Setälä, T., and Tenkanen, M. (2001) Overproduction, purification, and characterization of the *Trichoderma reesei* hydrophobin HFBI, *Appl. Microbiol. Biotechnol. 57*, 124−130.
44. Baldwin, R. (1986) Temperature dependence of the hydrophobic interaction in protein folding, *Proc. Natl. Acad. Sci. U.S.A. 83*, 8069−8072.
45. Lesk, A. (2003) Hydrophobicity − getting into hot water, *Biophys. J. 105*, 179−182.
46. Schellman, J. (1997) Temperature, stability, and the hydrophobic interaction, *Biophys. J. 73*, 2960−2964.
47. Berman, H. M., Westbrook, J., Feng, Z., Gilliland, G., Bhat, T. N., Weissig, H., Shindyalov, I. N., and Bourne, P. E. (2000) The protein data bank, *Nucleic Acids Res. 28*, 235−242.
48. DeLano, W. L. (2002) The PyMOL Molecular Graphics System, DeLano Scientific, San Carlos, CA.
49. Hakanpää, J., Szilvay, G. R., Kaljunen, H., Maksimainen, M., Linder, M., and Rouvinen, J. (2006) Two crystal structures of *Trichoderma reesei* hydrophobin HFBI: The structure of a protein amphiphile with and without detergent interaction, *Protein Sci.*, in press.

BI060620Y